A multiplexable assay for screening antibiotic lethality against drug-tolerant bacteria

Jonathan M. Stokes[1,2,8], Arnaud Gutierrez [1,2,3,8], Allison J. Lopatkin[1,2,4], Ian W. Andrews[1,2,4], Shawn French [5], Ivan Matic[3,6], Eric D. Brown[5] and James J. Collins [1,2,4,7]*

Antibiotic screens typically rely on growth inhibition to characterize compound bioactivity—an approach that cannot be used to assess the bactericidal activity of antibiotics against bacteria in drug-tolerant states. To address this limitation, we developed a multiplexed assay that uses metabolism-sensitive staining to report on the killing of antibiotic-tolerant bacteria. This method can be used with diverse bacterial species and applied to genome-scale investigations to identify therapeutic targets against tolerant pathogens.

The widespread dissemination of untreatable bacterial infections, combined with a lack of productivity in the discovery of new antibiotics, has created a global health crisis[1]. A substantial contributor to the failures in identifying novel functional classes of antibiotics is the lack of multiplexable methods that interrogate bacterial susceptibility to drugs beyond conventional growth inhibition approaches[2]. Indeed, while growth inhibition assays are methodologically simple and readily amenable to systems-level investigations, they have a number of shortcomings. First, these methods necessitate bacterial growth to acquire assay signal, which limits investigations to permissive growth conditions that might not accurately reflect the physiology of bacteria at infection sites[3]. In vivo environments can be resource-limited and induce diverse cellular states, including those that result in antibiotic tolerance[4–6]. Second, growth inhibition methods do not inform on whether treatments kill bacteria or prevent growth without cell death[7], the former of which is essential for the successful eradication of metabolically restricted, antibiotic-tolerant cells. Given that antibiotic tolerance plays a critical role in bacterial infections[6], there is an urgent need to develop methods for the rapid characterization of antibiotic-induced killing of tolerant bacteria.

In this study, we present the solid media portable cell killing (SPOCK) assay, a multiplexed method that uses metabolism-sensitive staining to report on the killing of antibiotic-tolerant bacteria residing in colonies. In addition to showing that the SPOCK assay can be used with a wide spectrum of bacterial species, we conducted genome-wide screens of the *Escherichia coli* Keio collection[8] using the antibiotic ciprofloxacin (CIP), which revealed unexplored adjuvant targets for this antibiotic against tolerant bacteria.

We hypothesized that we could generate a systems-level method capable of reporting on the bactericidal activity of antibiotics against bacteria in tolerant states by first growing mature colonies on nitrocellulose membranes to accumulate stationary phase, antibiotic-tolerant

cells, then transferring these mature colonies to environments where killing could be induced, and lastly monitoring bacterial cell death with a chemical indicator (Fig. 1a). We note that the use of colonies grown on membranes, rather than liquid cultures, provides a powerful method to study intrinsically antibiotic-tolerant cells with physiological diversity, and allows biomass accumulation and antibiotic exposure to occur in discrete environments.

To test this general design, we initially sought to understand the basic phenotypes of *E. coli* growth and killing on nitrocellulose membranes. We established the growth kinetics of *E. coli* colonies on nitrocellulose (Fig. 1b), and assayed for density-dependent CIP activity[9,10] (Fig. 1c and Supplementary Fig. 1a,b). As with *E. coli* grown in liquid culture (Fig. 1d,e), increased colony maturity correlated with decreased killing by CIP (Fig. 1c and Supplementary Fig. 1a,b). Furthermore, mature *E. coli* colonies showed tolerance to functionally diverse antibiotics (Fig. 1f, top and Supplementary Fig. 1c–e), confirming the loss of the bactericidal action of many drugs capable of killing metabolically active cells. We observed that two β-lactams, ampicillin (Amp) and cefsulodin (Cef), which both inhibit penicillin-binding protein 1a (PBP1a) and PBP1b[11], retained bactericidal capabilities against mature *E. coli* colonies (Fig. 1f, top), suggesting an active role for these enzymes in stationary phase cell survival within colonies.

We next substituted the time-consuming colony-forming unit (CFU) quantification procedure with metabolism-sensitive staining of colonies as a proxy for cell viability[12], with the goal of increasing assay throughput to a degree amenable to systems-level investigations. Here we used 2,3,5-triphenyl-2H-tetrazolium chloride (TTC), a common[13] redox-sensitive dye that is reduced to 1,3,5-triphenylformazan (TPF) in respiring cells, a precipitate that stains live colonies red (Fig. 1a).

We validated this metabolism-sensitive staining approach using both antibiotics (Fig. 1f, bottom and Supplementary Fig. 1e) and heat treatment at 80°C (Fig. 1g) to kill colony-embedded cells. We observed that killing of approximately 2 logs by heat treatment resulted in high colony autofluorescence (Fig. 1g), similar to that seen with killing by Amp and Cef (Fig. 1f). We applied colony staining using the reduction of TTC to TPF to a wide phylogenetic spectrum of heat-killed bacterial pathogens, as well as under conditions that perturbed cellular respiration (Supplementary Fig. 1f,g). These experiments show that the SPOCK assay can be broadly applied to clinically relevant pathogens residing in antibiotic-tolerant states

[1]Institute for Medical Engineering & Science, Department of Biological Engineering, and Synthetic Biology Center, Massachusetts Institute of Technology, Cambridge, MA, USA. [2]Infectious Disease and Microbiome Program, Broad Institute, Cambridge, MA, USA. [3]Inserm U1001, Faculté de Médecine Paris Descartes, Université Paris Descartes, Sorbonne Paris Cité, Paris, France. [4]Wyss Institute for Biologically Inspired Engineering, Harvard University, Boston, MA, USA. [5]Michael G. DeGroote Institute for Infectious Disease Research, Department of Biochemistry & Biomedical Sciences, McMaster University, Hamilton, Ontario, Canada. [6]Department of Life Sciences, Centre National de la Recherche Scientifique, Paris, France. [7]Harvard-MIT Program in Health Sciences and Technology, Cambridge, MA, USA. [8]These authors contributed equally: Jonathan M. Stokes, Arnaud Gutierrez. *e-mail: jimjc@mit.edu
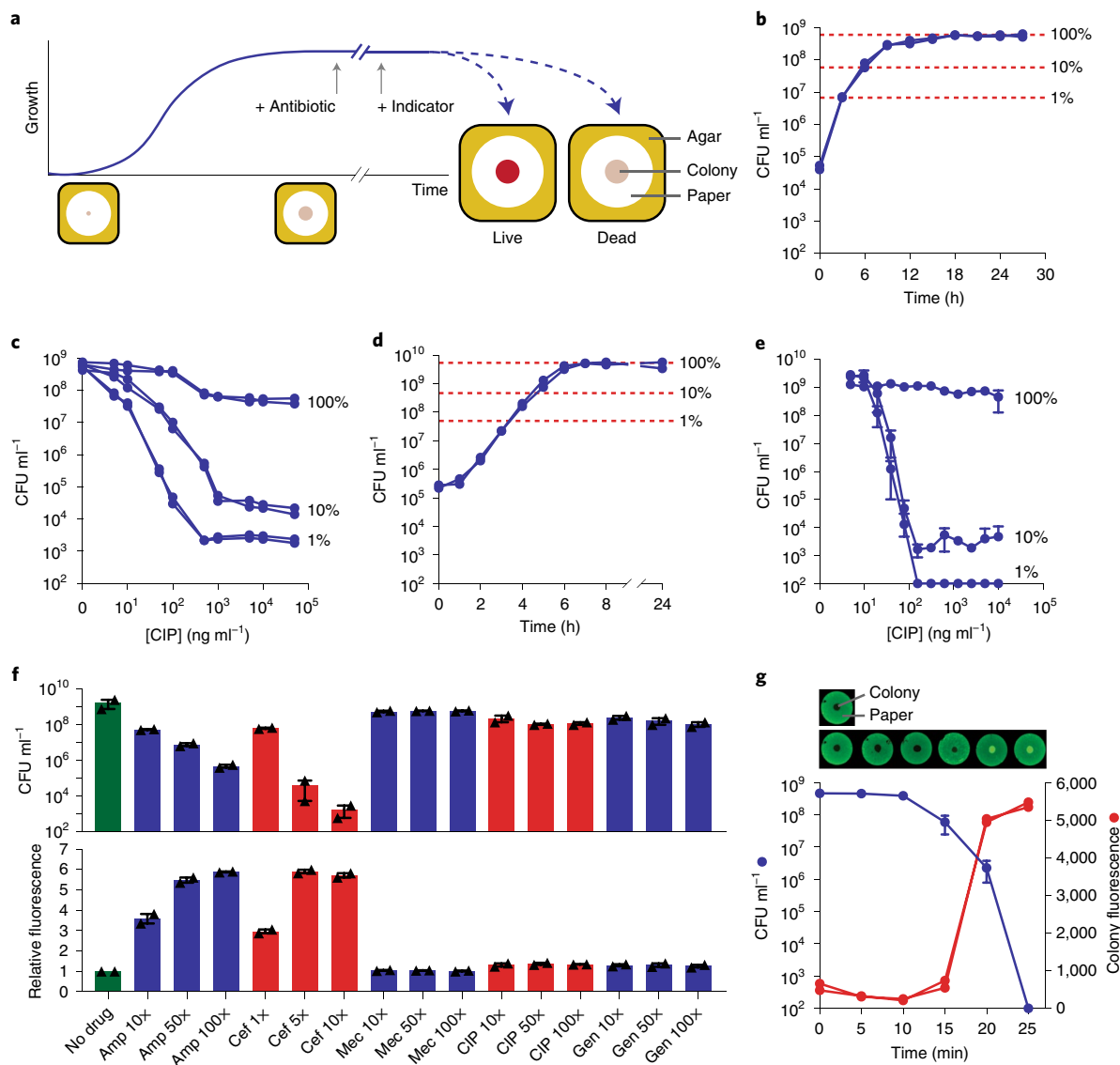
Fig. 1 | Basic principles of the SPOCK assay. a, Schematic of the SPOCK assay. Refer to the Methods for more details. **b**, Growth curve of wild-type *E. coli* colonies on nitrocellulose membranes growing on LB medium ($n = 2$ biologically independent experiments). The dashed red lines show the densities at which cells were sampled in **c**. **c**, Killing of wild-type *E. coli* colonies by CIP, where colonies were pre-grown on nitrocellulose to 1, 10, or 100% of maximum density on LB medium before transfer onto LB supplemented with CIP ($n = 2$ biologically independent experiments). **d**, Growth curve of wild-type *E. coli* in liquid LB medium ($n = 2$ biologically independent experiments). The dashed red lines show the densities at which cells were sampled in **e**. **e**, Killing of wild-type *E. coli* by CIP, where liquid cultures were grown to 1, 10, or 100% of maximum density in LB before adding CIP (mean ± s.d.; $n = 3$ biologically independent experiments). **f**, Killing of mature wild-type *E. coli* colonies by diverse antibiotics (top panel: mean ± range; $n = 2$ biologically independent experiments). Mec, mecillinam; Gen, gentamicin. The numbers show the fold-MIC concentrations used. Amp, Cef, Mec, CIP, and Gen are regarded as bactericidal against *E. coli*. The bottom panel shows the metabolic staining of wild-type *E. coli* colonies after treatment with the corresponding antibiotics on the top (mean ± range; $n = 2$ biologically independent experiments). **g**, Killing of mature wild-type *E. coli* colonies by heat treatment at 80 °C. Membranes were incubated for the noted durations, at which time these were assayed for CFU quantification (mean ± s.d.; $n = 4$ biologically independent experiments) or TTC staining ($n = 2$ biologically independent experiments). Example images of colony fluorescence are shown.

and used to report on the activity of bactericidal agents in diverse environments.

After validating TTC staining as being capable of reporting on the viability of bacteria in colonies, we used the SPOCK assay to conduct a genome-scale screen of the *E. coli* Keio collection[8]. Our aim was to demonstrate the utility of this method in identifying unexplored adjuvant targets that enhance the killing efficacy of antibiotics—in this instance, CIP—against tolerant cells. In this study, the Keio collection was seeded onto nitrocellulose membranes and grown to stationary phase. Membranes containing these mature colonies were

then transferred to medium supplemented with CIP. After antibiotic exposure, membranes were transferred to medium supplemented with TTC (Fig. 2a and Supplementary Fig. 2). On completion of colony staining, we imaged membranes for green fluorescence and observed autofluorescence of colonies consisting predominantly of dead cells, and masking of colonies containing cells that had tolerated CIP treatment (Fig. 2b and Supplementary Fig. 3a–d). We quantified the fluorescence intensities of colonies using a custom image analysis pipeline in MATLAB (MathWorks), and identified strains sensitive to killing by CIP (Supplementary Table 1).
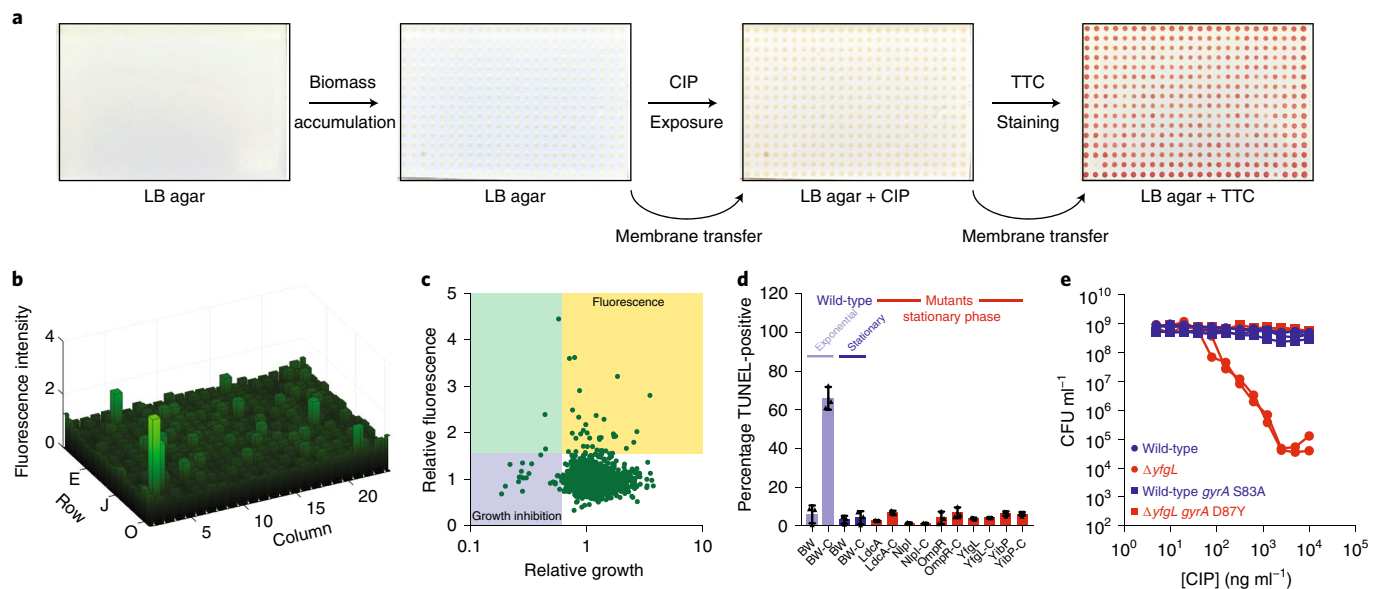
Fig. 2 | Screening the *E. coli* Keio collection for sensitivity to killing and growth inhibition by CIP. a, Summary of the genome-scale colony growth and killing protocol. Overnight cultures of all strains in the *E. coli* Keio collection were seeded onto nitrocellulose membranes, which were placed onto LB medium and incubated until stationary phase. Nitrocellulose membranes containing mature colonies were then transferred to LB medium supplemented with CIP and incubated. CIP-treated colonies were then transferred to LB medium supplemented with TTC to stain live colonies. **b**, Three-dimensional representation of colony fluorescence intensities on the example plate shown in **a**. **c**, Functional relationship between strains that are sensitive to killing by CIP under resource-depleted conditions (yellow), strains that are sensitive to growth inhibition under conventional assay conditions (blue), and strains that are sensitive in both conditions (green). **d**, Double-strand DNA breaks induced in wild-type *E. coli* by CIP during exponential growth (light blue) and stationary phase (dark blue). For exponential phase experiments, cells were treated with CIP (–C) or vehicle for 1 h before TUNEL analysis (mean ± s.d.; $n = 3$ biologically independent experiments). For stationary phase experiments, cells were treated with CIP (–C) or vehicle for 24 h before TUNEL analysis (mean ± s.d.; $n = 3$ biologically independent experiments). Shown in red are the stationary phase TUNEL data for gene deletion mutants that were identified as sensitive to killing by CIP in the SPOCK assay (mean ± s.d.; $n = 3$ biologically independent experiments). **e**, Sensitivity of wild-type *E. coli*, *ΔyfgL*, and CIP-resistant variants to killing by CIP in stationary phase (mean ± range; $n = 2$ biologically independent experiments). Wild-type *E. coli* (blue circles); *ΔyfgL E. coli* (red circles); wild-type harboring *gyrA* S83A (blue squares); *ΔyfgL* harboring *gyrA* D87Y (red squares).

Strains with fluorescence values 3σ or greater than the mean of the entire Keio collection were classified as hits (Fig. 2c, Supplementary Fig. 3d, and Supplementary Table 2). We identified a total of 38 strains as being sensitive to killing by CIP. Notably, on classification of these hit strains, we observed a lack of gene deletion mutants that are known to conventionally confer sensitivity to quinolones[7], thus providing evidence that deletions causing sensitivity during active growth diverge from those in metabolically restricted states. Rather, the SPOCK assay enriched for single-gene deletions that affect cell envelope composition, as well as carbohydrate and nucleotide biosynthesis (Supplementary Table 3), revealing an uncharted functional set of deletions that confer CIP sensitivity.

To further demonstrate the utility of the SPOCK assay in identifying adjuvant targets that would be overlooked by standard methods, we performed a conventional growth inhibition screen of the Keio collection against CIP (Fig. 2d, Supplementary Fig. 3e–g, and Supplementary Table 1). We acquired 27 hit strains, which were enriched for gene deletion mutants deficient in DNA damage repair, in agreement with prior work[7] (Supplementary Tables 4 and 5). Only four strains across the Keio collection showed sensitivity to CIP in both resource-limited colonies and under permissive growth conditions, thus highlighting the lack of functional redundancy between these two approaches.

We next sought to understand whether hit strains identified by the SPOCK assay could help inform on unexplored biological processes governing CIP bioactivity. We first validated that the hit strains from the SPOCK assay did not display enhanced sensitivity to CIP by using minimum inhibitory concentration (MIC) testing (Supplementary Fig. 4a) and confirmed their sensitivity to killing by CIP in stationary phase liquid cultures (Supplementary Fig. 4b–e).

Next, we selected a subset of gene deletion mutants that showed sensitivity to killing by CIP under resource-depleted conditions for analysis of CIP-induced DNA damage—namely *ΔldcA*, *ΔnlpI*, *ΔompR*, *ΔyfgL*, and *ΔyibP*—all of which are involved in cell envelope homeostasis (Supplementary Figs. 5 and 6). We quantified DNA damage[14] during exponential phase (Supplementary Fig. 7a,b) and confirmed CIP-induced DNA damage in all strains. We then analyzed DNA damage in cells that were grown to stationary phase before CIP treatment (Fig. 2d and Supplementary Fig. 7a). We did not observe increased DNA damage in any gene deletion mutant after CIP treatment, despite increased sensitivity to killing. Consistently, resource-depleted stationary phase cells did not display antibiotic-induced morphologies common to growing cells[15] (Supplementary Fig. 7c–h).

We next asked whether chromosomal mutations that inhibit CIP binding to DNA gyrase would confer stationary phase tolerance in the *ΔyfgL* background, which we selected for its high sensitivity to killing. To this end, we isolated a CIP-resistant mutant in wild-type *E. coli* (*gyrA* S83A) and *ΔyfgL E. coli* (*gyrA* D87Y). Both mutations resulted in an eightfold increase in MIC relative to that of parental strains (Supplementary Fig. 7i,j), and identical dose–response profiles of killing during exponential growth (Supplementary Fig. 7k). Additionally, neither *gyrA* mutation caused growth defects (Supplementary Fig. 7l,m). We observed that the *gyrA* D87Y mutation in the *ΔyfgL* strain conferred wild-type levels of tolerance to CIP in stationary phase (Fig. 2e). Collectively, these data suggest that in stationary phase *ΔyfgL* cells, CIP was bactericidal through binding of DNA gyrase, but induced downstream molecular events that diverged from those seen in metabolically active states. Although the

specific underlying mechanism remains to be identified, these findings highlight the value of the SPOCK assay in providing new insight into the response of antibiotic-tolerant bacteria to antibiotics.

Current systems-level methods to study antibiotic activity have largely been limited to analysis of the growth of cells in nutrient-replete conditions[1]. This lack of appropriate methods has restricted the ability to develop effective antibiotics against resource-limited, antibiotic-tolerant infections. In this study, we present the SPOCK assay as a multiplexable tool that applies TTC staining to probe antibiotic-induced killing of tolerant bacteria in the context of resource-depleted mature colonies. Notably, redox-sensitive dyes have been widely applied to monitor the metabolic potential of eukaryotic and bacterial species[13]. For instance, previous investigations dating back more than three decades used TTC to quantify the killing of *E. coli* by non-antibiotic biocides[16], and more contemporary work applied a related tetrazolium salt, sodium 3′-[1-[(phenylamino)-carbony]-3,4-tetrazolium]-bis(4-methoxy-6-nitro)benzene-sulfonic acid hydrate, to determine the MICs of bactericidal antibiotics against *Pseudomonas aeruginosa*[17]. However, where these and other[18–20] approaches were limited to the analysis of metabolically active cells undergoing growth in homogeneous liquid cultures, the SPOCK assay expands on these experimental designs considerably by affording the capability of monitoring the death of phenotypically heterogeneous bacteria in metabolically restricted, antibiotic-tolerant colonies. Furthermore, because the SPOCK assay allows for cells to be grown, treated with antibiotics, and stained in discrete environments in a multiplexed fashion, users can carry out genome-scale analyses of antibiotic-tolerant cell killing with precise modulation of colony growth and antibiotic exposure durations, as well as with drug treatments occurring in restrictive conditions.

Overall, the SPOCK assay will serve as a valuable tool to broaden the currently limited understanding of mechanisms to enhance antibiotic efficacy against tolerant bacteria. Furthermore, this method holds promise for providing novel insights into how the manipulation of bacterial metabolic state governs bactericidal antibiotic efficacy. We posit that when coupled with conventional growth inhibition approaches, the SPOCK assay will serve to reveal a comprehensive set of targets for treating bacteria in diverse metabolic states.

Online content

Any methods, additional references, Nature Research reporting summaries, source data, statements of data availability and associated accession codes are available at https://doi.org/10.1038/s41592-019-0333-y.

References

1. Brown, E. D. & Wright, G. D. *Nature* **529**, 336–343 (2016).
2. Wiegand, I., Hilpert, K. & Hancock, R. E. W. *Nat. Protoc.* **3**, 163–175 (2008).
3. Certain, L. K., Way, J. C., Pezone, M. J. & Collins, J. J. *Cell Host Microbe* **22**, 263–268 (2017).
4. Cornforth, D. M. et al. *Proc. Natl Acad. Sci. USA* **115**, E5125–E5134 (2018).
5. Brauner, A., Fridman, O., Gefen, O. & Balaban, N. Q. *Nat. Rev. Microbiol.* **14**, 320–330 (2016).
6. Meylan, S., Andrews, I. W. & Collins, J. J. *Cell* **172**, 1228–1238 (2018).
7. Liu, A. et al. *Antimicrob. Agents Chemother.* **54**, 1393–1403 (2010).
8. Baba, T. et al. *Mol. Syst. Biol.* **2**, 2006.0008 (2006).
9. Gutierrez, A. et al. *Mol. Cell* **68**, 1147–1154.e3 (2017).
10. Gutierrez, A., Stokes, J. M. & Matic, I. *Antibiotics (Basel)* **7**, 32 (2018).
11. Sarkar, S. K., Dutta, M., Kumar, A., Mallik, D. & Ghosh, A. S. *PLoS ONE* **7**, e48598 (2012).
12. Asadishad, B., Ghoshal, S. & Tufenkji, N. *Environ. Sci. Technol.* **45**, 8345–8351 (2011).
13. Berridge, M. V., Herst, P. M. & Tan, A. S. *Biotechnol. Annu. Rev.* **11**, 127–152 (2005).
14. Rohwer, F. & Azam, F. *Appl. Environ. Microbiol.* **66**, 1001–1006 (2000).
15. Michel, B. *PLoS Biol.* **3**, e255 (2005).
16. Hurwitz, S. J. & McCarthy, T. J. *J. Pharm. Sci.* **75**, 912–916 (1986).
17. Tunney, M. M., Ramage, G., Field, T. R., Moriarty, T. F. & Storey, D. G. *Antimicrob. Agents Chemother.* **48**, 1879–1881 (2004).
18. Fleck, L. E. et al. *Antimicrob. Agents Chemother.* **58**, 1410–1419 (2014).
19. Shea, A., Wolcott, M., Daefler, S. & Rozak, D. A. *Methods Mol. Biol.* **881**, 331–373 (2012).
20. Mackie, A. M., Hassan, K. A., Paulsen, I. T. & Tetu, S. G. *Methods Mol. Biol.* **1096**, 123–130 (2014).

Author contributions

J.M.S. and A.G. conceptualized the study. J.M.S., A.G., A.J.L., I.W.A., and S.F. carried out the data acquisition and analysis. J.M.S. and A.G. wrote the manuscript. J.M.S., A.G., A.J.L., I.W.A., S.F., E.D.B., and J.J.C. edited the manuscript. J.M.S., A.G., I.M., E.D.B., and J.J.C. acquired the funding. I.M., E.D.B., and J.J.C. supervised the work.

Competing interests

J.J.C. is scientific cofounder and SAB chair of EnBiotix, an antibiotic drug discovery company.

Additional information

Supplementary information is available for this paper at https://doi.org/10.1038/s41592-019-0333-y.

Reprints and permissions information is available at www.nature.com/reprints.

Correspondence and requests for materials should be addressed to J.J.C.

Publisher's note: Springer Nature remains neutral with regard to jurisdictional claims in published maps and institutional affiliations.

Methods

Growth and killing of bacterial colonies by CIP on nitrocellulose membranes. Overnight cultures of *E. coli* BW25113, the parent strain of the *E. coli* collection[8], were grown from frozen stocks in 3 ml of liquid lysogeny broth (LB) medium overnight at 37 °C with shaking at 300 r.p.m. (INFORS HT Multitron Pro). Subsequently, 0.1 µl of culture was seeded onto 13-mm nitrocellulose disks (catalog no. GSWP01300; Millipore Sigma), which were placed onto solid LB agar, and grown to the required density at 37 °C. Using sterile forceps (11151-10; Fine Science Tools), we transferred the disks to solid LB agar supplemented with CIP (catalog no. 17850; Sigma-Aldrich), prepared in 0.1 M NaOH, and incubated them at 37 °C for 24 h. After antibiotic treatment, disks were transferred to solid LB agar supplemented with 50 µg ml⁻¹ TTC (catalog no. ab145043; Abcam), freshly prepared in deionized H$_2$O, and incubated at 37 °C for 1 h. After colony staining, disks were imaged at excitation and emission wavelengths for Cy3 using an Azure c400 imaging system (Azure Biosystems) to differentiate live and dead cells on the basis of autofluorescence of *E. coli* colonies. Specifically, live cells stained red owing to their ability to reduce TTC to TPF, whereas dead cells did not stain and therefore emitted green fluorescence. Although this change in colony color could be observed by eye, we reasoned that the intrinsic green autofluorescence displayed by *E. coli* cells[21], which is masked by TPF accumulation in respiring colonies, would provide a more robust signal to differentiate dead colonies from live ones. We note that the autofluorescence of *E. coli* is in the same wavelength range as Cy3. For instances where CFUs were quantified, rather than transferring antibiotic-treated disks to LB agar supplemented with TTC, we submerged disks in 1 ml of sterile PBS (catalog no. 46-013-CM; Corning) in microcentrifuge tubes (catalog no. 1615-5500; Seal-Rite) and vortexed them at 3,000 r.p.m. for 30 min. Cells were then tenfold serially diluted in sterile PBS, plated onto solid LB agar, and incubated overnight at 37 °C. For instances where the colony area was calculated, colony edges were detected using a custom MATLAB script in ImageJ (NIH), and the number of pixels within each was determined. The number of pixels within each 13-mm disk was also determined, and the areas of colonies in mm² were calculated using the known area of the disk as a pixel-scaling factor. Potassium cyanide was purchased from Sigma-Aldrich (catalog no. 60178).

Growth and killing of bacterial colonies by heat on nitrocellulose membranes. For the heat treatment experiments, overnight cultures of *E. coli* BW25113 were grown as described earlier, seeded onto nitrocellulose disks, and grown for 24 h on solid LB agar at 37 °C. Disks were subsequently removed from solid LB medium, placed into empty sterile petri dishes (catalog no. 351029; Corning), and incubated at 80 °C for the noted durations in a Gravity Convention Oven (VWR). Disks were either stained with TTC or plated for CFU quantification as described earlier. All pathogens were grown and treated as described for *E. coli* BW25113, except that membranes were incubated at 80 °C for 30 min before staining or plating. The *Klebsiella pneumoniae*, *Acinetobacter baumannii*, *P. aeruginosa*, *Staphylococcus aureus*, and *Enterococcus faecalis* strains shown in Supplementary Fig. 1g are de-identified clinical isolates from Brigham and Women's Hospital. The *Enterobacter cloacae* strain shown in Supplementary Fig. 1g is a de-identified clinical isolate from the Massachusetts General Hospital. *Bacillus simplex* is an environmental isolate from the Massachusetts General Hospital. The *Mycobacterium smegmatis* strain MC² 155 was acquired from the D. Hung laboratory.

Screening of the *E. coli* Keio collection for sensitivity to killing by CIP. All strains of the *E. coli* Keio collection were pinned from frozen stocks into liquid LB medium supplemented with 50 µg ml⁻¹ kanamycin sulfate (catalog no. 60615; Sigma-Aldrich) in 384-density in a final volume of 40 µl. Plates were incubated at 37 °C overnight until saturation, at which time strains were pinned onto 8 × 12 cm nitrocellulose membranes (catalog no. 77012; Thermo Fisher Scientific), which had been placed onto solid LB agar in PlusPlates (Singer Instruments). Pinning was conducted using a Singer ROTOR automated pinning system (Singer Instruments). Plates were incubated at 37 °C for 24 h until all colonies reached maturation, at which time membranes were transferred with sterile forceps to LB agar supplemented with 1 µg ml⁻¹ CIP (100 × MIC) and incubated for an additional 24 h at 37 °C. A no-treatment control screen was conducted in parallel, where colonies were transferred to LB without CIP. After CIP treatment, membranes were transferred to LB agar supplemented with 50 µg ml⁻¹ TTC and incubated at 37 °C for 1 h. After colony staining, membranes were fluorescently imaged at excitation and emission wavelengths for Cy3 using an Azure c400 imaging system to differentiate live and dead colonies based on the intrinsic fluorescence properties of *E. coli*. Membrane images were then analyzed using a custom image analysis pipeline in MATLAB. Imported .tif files were first converted to gray scale and then binarized using the Otsu's global image threshold to locate the placement of the nitrocellulose membrane. Because the location and angle of the membrane varied slightly between each image, rotational and spatial transformations were normalized to a rectangular grid aligned with the membrane. A Hough transform was used to detect all colonies within this region and simple morphological operations were performed to eliminate small particles and image noise. To filter any remaining technical artifacts, such as slight membrane creasing, we placed a 16 × 24 grid within the determined rectangular region to identify coordinates with one, more than one, or zero colonies present. Exactly one colony per grid

coordinate was determined on the basis of the relative size and placement of all detected circles within an individual square (nearest to the center). Because the outline of killed colonies could be detected by fluorescence imaging, if no colony satisfied our defined criteria, the grid coordinate was designated as empty owing to technical error. A colony mask was then generated within the nitrocellulose coordinates and the average intensity of the complement of this mask (for example, nitrocellulose membrane without the colonies) was used to adjust the background of each image. Finally, background-adjusted colony intensities were normalized by row, column, and plate averages to account for edge- and image-specific fluorescence effects. Colonies were then sorted by the corresponding Keio collection gene list and average intensities were compared between experiments. For all image analyses, image processing was used only to generate image masks where designated. Raw images within the masked regions were used for all data quantification. Once fluorescence intensities had been calculated for each strain, CIP-treated sample fluorescence values were divided by the corresponding values for their untreated controls to obtain a fold change in strain sensitivity to CIP.

Screening of the *E. coli* Keio collection for sensitivity to growth inhibition by CIP. All strains of the *E. coli* Keio collection were pinned from frozen stocks into liquid LB medium supplemented with 50 µg ml⁻¹ kanamycin in 384-density in a final volume of 40 µl. Plates were incubated at 37 °C overnight until saturation, at which time strains were seeded into fresh LB supplemented with 1/8 × MIC CIP at a density of approximately 10⁶ CFU ml⁻¹, in 384-density. In parallel, strains were seeded into fresh LB without CIP. Plates were then incubated for 18 h at 37 °C, after which optical density (600 nm) was read using a Tecan Infinite M1000 microplate reader. Optical density values were normalized by row, column, and plate as described earlier to account for spatial effects on each plate, as well as plate-to-plate variation. The optical densities of CIP-treated samples were divided by their untreated controls to obtain a fold change in strain sensitivity to CIP similar to that described earlier.

Gene ontology enrichment. Hit strains identified from the two screens of the *E. coli* Keio collection were classified according to Gene Ontology Consortium terms with EcoCyc pathway tools[22–24]. This list was further refined to include transcriptional regulation and biosynthetic pathways via an enrichment analysis in EcoCyc pathway tools. Quantification of the number of genes present in each Gene Ontology Consortium term, promoter activation class, or biosynthetic pathway were compiled, along with *P* values calculated using Fisher's exact test, to assess the statistical enrichment of cellular processes for sensitivity to CIP bioactivity.

Analysis of killing and growth inhibition by CIP in liquid culture. For sensitivity to killing by CIP, gene deletion mutants from the Keio collection were grown from frozen stocks in 3 ml of liquid LB medium supplemented with 50 µg ml⁻¹ kanamycin overnight at 37 °C with shaking at 300 r.p.m. These cultures were then subcultured 1/10,000 into 100 µl of fresh LB medium in 96-well round bottom plates (catalog no. CLS3788; Corning) and incubated at 37 °C with shaking at 900 r.p.m. for 24 h until saturation. Cultures were then treated with the noted concentration(s) of CIP and incubated at 37 °C with shaking at 900 r.p.m. for an additional 24 h. Cells were then collected and washed in sterile PBS, and serially diluted tenfold in sterile PBS before being plated onto solid LB agar. After overnight incubation, the CFUs for each condition were calculated. In Supplementary Fig. 4d, relative survival is calculated as the ratio of the survival of wild-type *E. coli* BW25113 to the survival of each gene deletion mutant in the presence of 1 µg ml⁻¹ CIP. For sensitivity to growth inhibition by CIP, strains were grown from frozen stocks in 3 ml of liquid LB medium supplemented with 50 µg ml⁻¹ kanamycin overnight at 37 °C with shaking at 300 r.p.m. These cultures were then subcultured 1/10,000 into fresh LB medium and incubated with varying concentrations of CIP in a final volume of 100 µl at 37 °C with shaking at 900 r.p.m. in 96-well round bottom microtiter plates. When untreated control cultures reached stationary phase, plates were read at 600 nm with a SpectraMax M3 Plate Reader (Molecular Devices). For growth kinetics analyses, strains were grown from frozen stocks in 3 ml of liquid LB medium supplemented with 50 µg ml⁻¹ kanamycin overnight at 37 °C with shaking at 300 r.p.m. These cultures were then subcultured 1/10,000 into fresh LB medium and incubated in a final volume of 100 µl at 37 °C with shaking in 96-well round bottom microtiter plates using a SpectraMax M3 Plate Reader. Optical density at 600 nm was measured every 10 min over 24 h.

DNA damage analysis using terminal deoxynucleotidyl transferase dUTP nick end labeling (TUNEL). Cells were grown from frozen stocks in 3 ml of liquid LB medium supplemented with 50 µg ml⁻¹ kanamycin overnight at 37 °C with shaking at 220 r.p.m. These cultures were then subcultured 1/10,000 into 25 ml of fresh LB in a 250-ml baffled flask and grown at 37 °C with shaking at 220 r.p.m. Cells were collected at an optical density of approximately 0.1, or after 24 h of incubation, for exponential and stationary phase analyses, respectively. After the required incubation period, 1 ml of cells were transferred to a 14-ml conical vial and treated with 100 ng ml⁻¹ CIP for 1 h (exponential phase) or 1 µg ml⁻¹ CIP for 24 h (stationary phase). Untreated control cultures were assayed in parallel for both sets of experiments. We used hydrogen peroxide (100 mM) as a positive control

by treating exponential cultures for 10 min. After treatment, approximately 10^7 cells were collected and washed three times in ice-cold PBS, followed by fixation in fresh 0.4% (v/v) paraformaldehyde in PBS for 20 min. Cells were then washed again three times in ice-cold PBS and permeabilized with 0.4% (v/v) Triton X-100 in PBS. Cells were then washed three times in ice-cold PBS. The TUNEL reaction was done using the DeadEnd Fluorometric TUNEL System (Promega). Cells were mixed in the dark with the enzyme-nucleotide-buffer solution and incubated for 1 h at 37 °C. The reaction was terminated by adding 1 ml of 20 mM EDTA; the TUNEL signal was quantified with a Gallios Flow Cytometer (Beckman Coulter).

Fluorescence microscopy. Cells were grown from frozen stocks in 3 ml of liquid LB medium supplemented with 50 µg ml⁻¹ kanamycin overnight at 37 °C with shaking at 300 r.p.m. These cultures were then subcultured 1/10,000 into 25 ml of fresh LB in a 250-ml baffled flask and grown at 37 °C with shaking at 300 r.p.m. Cells were collected at an optical density of approximately 0.1, or after 24 h of incubation, for exponential and stationary phase analyses, respectively. After the required pretreatment incubation period, 1 ml of cells were transferred to a 14-ml conical vial and treated with 100 ng ml⁻¹ CIP for 24 h (exponential phase) or 1 µg ml⁻¹ CIP for 24 h (stationary phase). Untreated control cultures were assayed in parallel. For all samples, after the described CIP incubation period, 1 µl of culture was removed and added to 100 µl of ice-cold 1.5% glutaraldehyde in PBS. After overnight fixation at 4 °C in a dark environment, cells were stained with FM 4-64 dye (1 µg ml⁻¹; Thermo Fisher Scientific) at room temperature in the dark for 5 min and imaged with a Nikon Ti-E inverted microscope with excitation from a Lumencor Sola LED illuminator (Lumencor). Images were captured with an ORCA-Flash 4.0 camera (Hamamatsu).

Resistant mutant generation and sequencing. Cells were grown from frozen stocks in 3 ml of liquid LB medium supplemented with 50 µg ml⁻¹ kanamycin overnight at 37 °C with shaking at 300 r.p.m. Approximately 10^8 cells were then inoculated onto solid LB supplemented with 50 µg ml⁻¹ kanamycin (for the Keio strains) and 16 µg ml⁻¹ nalidixic acid to maximize mutations exclusively in *gyrA*. Plates were then incubated at 37 °C for 48–72 h, and individual colonies were isolated and grown in liquid LB supplemented with 50 µg ml⁻¹ kanamycin (for the Keio strains) and 50 ng ml⁻¹ CIP. Mutations in

gyrA were initially identified using Sanger sequencing. The *gyrA* gene was amplified using the forward 5′-CGGCGATTTTTCGGCATTCA-3′ and reverse 5′-GGCACAGCCAAACTTTACCG-3′ primers. *E. coli* BW25113, Δ*yfgL*, and a single CIP-resistant mutant in each parental background were subsequently selected for whole-genome sequencing. CIP-resistant mutants were selected on the basis of their identical eightfold shift in CIP MIC relative to their respective parental backgrounds. Chromosomal DNA was purified using a Gentra Puregene kit (QIAGEN) according to the manufacturer's instructions and sequenced on a MiSeq platform (Illumina) before being aligned to the *E. coli* MG1655 reference genome (NC_000913) to verify the absence of additional mutations beyond those observed in *gyrA*.

Reporting Summary. Further information on research design is available in the Nature Research Reporting Summary linked to this article.

Code availability

The MATLAB code for the image analysis is available at https://github.com/ajlopatkin/spock-analysis-pipeline.

Data availability

Large screening datasets are provided as Supplementary Information in Supplementary Table 1. Sequencing data are available at the NCBI Sequence Read Archive under accession no. PRJNA517046. The source data for Figs. 1 and 2, and Supplementary Figs. 1, 2, and 4–7 are available online (source data for Supplementary Fig. 3 are available in Supplementary Table 1). Additional data that support the findings of this study are available from the corresponding author upon reasonable request.

References

21. Ammor, M. S. *J. Fluoresc.* **17**, 455–459 (2007).
22. Keseler, I. M. et al. *Nucleic Acids Res.* **41**, D605–D612 (2013).
23. Karp, P. D. et al. *Brief. Bioinform.* **17**, 877–890 (2016).
24. Karp, P. D. *Science* **293**, 2040–2044 (2001).

Corresponding author(s): James J. Collins

Reporting Summary

Nature Research wishes to improve the reproducibility of the work that we publish. This form provides structure for consistency and transparency in reporting. For further information on Nature Research policies, see Authors & Referees and the Editorial Policy Checklist.

Statistical parameters

When statistical analyses are reported, confirm that the following items are present in the relevant location (e.g. figure legend, table legend, main text, or Methods section).

n/a	Confirmed	
☐	☒	The exact sample size (*n*) for each experimental group/condition, given as a discrete number and unit of measurement
☐	☒	An indication of whether measurements were taken from distinct samples or whether the same sample was measured repeatedly
☐	☒	The statistical test(s) used AND whether they are one- or two-sided *Only common tests should be described solely by name; describe more complex techniques in the Methods section.*
☒	☐	A description of all covariates tested
☒	☐	A description of any assumptions or corrections, such as tests of normality and adjustment for multiple comparisons
☐	☒	A full description of the statistics including central tendency (e.g. means) or other basic estimates (e.g. regression coefficient) AND variation (e.g. standard deviation) or associated estimates of uncertainty (e.g. confidence intervals)
☐	☒	For null hypothesis testing, the test statistic (e.g. *F*, *t*, *r*) with confidence intervals, effect sizes, degrees of freedom and *P* value noted *Give P values as exact values whenever suitable.*
☒	☐	For Bayesian analysis, information on the choice of priors and Markov chain Monte Carlo settings
☒	☐	For hierarchical and complex designs, identification of the appropriate level for tests and full reporting of outcomes
☒	☐	Estimates of effect sizes (e.g. Cohen's *d*, Pearson's *r*), indicating how they were calculated
☐	☒	Clearly defined error bars *State explicitly what error bars represent (e.g. SD, SE, CI)*

Our web collection on statistics for biologists may be useful.

Software and code

Policy information about availability of computer code

Data collection	No custom software was used for data collection.
Data analysis	Code written in MATLAB was used to analyze plate images for colony fluorescence through Image J. This has been deposited to GitHub and is immediately available to readers. A detailed description of the function of the code, as well as a code availability statement, are found in Online Methods. EcoCyc version 21.0 was used for gene enrichment analysis.

For manuscripts utilizing custom algorithms or software that are central to the research but not yet described in published literature, software must be made available to editors/reviewers upon request. We strongly encourage code deposition in a community repository (e.g. GitHub). See the Nature Research guidelines for submitting code & software for further information.

Data

Policy information about availability of data

All manuscripts must include a data availability statement. This statement should provide the following information, where applicable:
- Accession codes, unique identifiers, or web links for publicly available datasets
- A list of figures that have associated raw data
- A description of any restrictions on data availability

All large-scale screening datasets are available in the supplemental information and/or from the corresponding author upon request.

Field-specific reporting

Please select the best fit for your research. If you are not sure, read the appropriate sections before making your selection.

☒ Life sciences   ☐ Behavioural & social sciences   ☐ Ecological, evolutionary & environmental sciences

For a reference copy of the document with all sections, see nature.com/authors/policies/ReportingSummary-flat.pdf

Life sciences study design

All studies must disclose on these points even when the disclosure is negative.

Sample size	Samples sizes for experiments were determined based on field convention, in independent biological duplicate or greater performed by different investigators on different days.
Data exclusions	No data was excluded from analysis.
Replication	At least two investigators performed experiments, after which data was compiled and analyzed. For stationary phase killing experiments that were performed on later dates as controls for additional experiments, data were within +/- 1 log of the original data.
Randomization	Given the nature of the experiments analyzing E. coli mutant sensitivity to antibiotics, randomization was not necessary.
Blinding	Genetic mutants were blinded using an alphanumeric code, which was not known to the investigator conducting the given experiment. Codes were then associated to the genetic mutation after data had been gathered.

Reporting for specific materials, systems and methods

Materials & experimental systems

n/a	Involved in the study
☒	☐ Unique biological materials
☒	☐ Antibodies
☒	☐ Eukaryotic cell lines
☒	☐ Palaeontology
☒	☐ Animals and other organisms
☒	☐ Human research participants

Methods

n/a	Involved in the study
☒	☐ ChIP-seq
☐	☒ Flow cytometry
☒	☐ MRI-based neuroimaging

Flow Cytometry

Plots

Confirm that:

☒ The axis labels state the marker and fluorochrome used (e.g. CD4-FITC).

☒ The axis scales are clearly visible. Include numbers along axes only for bottom left plot of group (a 'group' is an analysis of identical markers).

☒ All plots are contour plots with outliers or pseudocolor plots.

☒ A numerical value for number of cells or percentage (with statistics) is provided.

Methodology

Sample preparation	Cells were grown from frozen stocks in 3 ml of liquid LB media supplemented with 50 μg/ml kanamycin overnight at 37°C shaking at 220 rpm. These cultures were then subcultured 1/10,000 into 25 ml fresh LB in a 250 ml baffled flask and grown at 37°C shaking at 220 rpm. Cells were harvested at OD~0.1, or after 24 hours of incubation, for exponential phase and stationary phase analyses, respectively. After the required incubation period, 1 ml of cells were transferred to a 14 ml conical vial and treated with 100 ng/ml ciprofloxacin for one hour (exponential phase) or 1 μg/ml ciprofloxacin for 24 hours (stationary phase). Untreated control cultures were assayed in parallel for both sets of experiments. Hydrogen peroxide (100 mM) was used as a positive control by treating exponential cultures for ten minutes. After treatment, ~107 cells were collected and washed three times in ice-cold, PBS, followed by fixation in fresh 0.4% (v/v) paraformaldehyde in PBS for 20 minutes. Cells were then washed again three times in ice-cold, PBS and permeabilized with 0.4% (v/v) Triton X-100 in PBS. Cells were then washed three times in ice-cold, PBS. The TUNEL reaction was done using the DeadEnd Fluorometric TUNEL System (Promega). Here, cells were mixed in

the dark with the enzyme-nucleotide-buffer solution and incubated for one hour at 37°C. The reaction was terminated by adding 1 ml of 20 mM EDTA.

Instrument

TUNEL signal was quantified using a Beckman Coulter Gallios flow cytometer (Beckman Coulter).

Software

Flow cytometry data was collected and analyzed using Kaluza and FlowJo.

Cell population abundance

50,000 cells were analyzed for each sample.

Gating strategy

No gating strategy was applied. The entire cell population observed in the FSC/SSC plot was analyzed.

☒ Tick this box to confirm that a figure exemplifying the gating strategy is provided in the Supplementary Information.